Conserved use of the sodium/bile acid cotransporter (NTCP) as an entry receptor by hepatitis B virus and domestic cat hepadnavirus

Maya Shofa [1,2], Akiho Ohkawa [1], Yasuyuki Kaneko [1,3], Akatsuki Saito [1,2,4] *

[1]Department of Veterinary Science, Faculty of Agriculture, University of Miyazaki, Miyazaki, Miyazaki 8892192, Japan

[2]Graduate School of Medicine and Veterinary Medicine, University of Miyazaki, Miyazaki, Miyazaki 8891692, Japan

[3]Veterinary Teaching Hospital, Faculty of Agriculture, University of Miyazaki, Miyazaki, Miyazaki 8892192, Japan

[4]Center for Animal Disease Control, University of Miyazaki, Miyazaki, Miyazaki 8892192, Japan

*Corresponding author: Akatsuki Saito (sakatsuki@cc.miyazaki-u.ac.jp)

Abstract

The *Orthohepadnavirus* genus includes hepatitis B virus (HBV) that can cause chronic hepatitis and hepatocarcinoma in humans. Recently, a novel hepadnavirus in cats, domestic cat hepadnavirus (DCH), was identified that is genetically close to HBV. DCH infection is associated with chronic hepatitis in cats, suggesting a similarity with HBV pathogenesis and the potential to use DCH as a novel animal model for HBV research. HBV is shown to use the sodium/bile acid cotransporter (NTCP) as a major cell entry receptor, but the equivalent receptor for DCH remains unknown. Here we sought to identify the entry receptor for DCH. HBV- and DCH-derived preS1 peptides efficiently bound to both human and cat NTCPs, and residue 158 of NTCP proteins determined the species-specific binding of the DCH preS1 peptide. Myrcludex B, an HBV entry inhibitor, blocked binding of the DCH preS1 peptide. Thus, DCH and HBV may share cell entry molecules, suggesting a possibility of inter-species transmission. Furthermore, our study suggests that DHC can be useful as a novel model for HBV research.

Keywords: hepadnavirus, hepatitis B virus (HBV), domestic cat hepadnavirus, sodium/bile acid cotransporter (NTCP)

32 **1. Introduction**

33 *Hepadnaviridae* are enveloped DNA viruses that have a partially double-stranded, circular
34 DNA genome and a broad host tropism, including mammals, reptiles, frogs, birds, and fish (Magnius
35 et al., 2020). Human infection with hepatitis B virus (HBV), a member of *Orthohepadnavirus* genus,
36 can induce chronic liver damage, including cirrhosis and hepatocellular carcinoma, and, despite
37 effective vaccines being available, eradicating chronic infections can be challenging. Therefore,
38 suitable HBV animal models are required to advance therapeutic outcomes. Chimpanzees are now
39 unavailable as animal models for HBV infection, and infection models using HBV-like viruses in
40 woodchuck, ground squirrel, and duck have consequently been investigated (Delmas et al., 2002;
41 Guo et al., 2000; Jilbert et al., 1992; Kajino et al., 1994; Marion et al., 2002). Although treeshrews
42 (Tupaia) are used as an animal model, the limited availability of research reagents may make it
43 difficult to use this animal. Therefore, development of a novel and convenient animal model is still
44 required.

45 In 2018, an HBV-like virus, domestic cat hepadnavirus (DCH), was identified in domestic cats
46 in Australia and was associated with feline chronic hepatitis (Aghazadeh et al., 2018), suggesting a
47 similarity with HBV pathogenesis. Subsequently, DCH was identified in other countries, including
48 Italy (Lanave et al., 2019), Thailand (Piewbang et al., 2020), Malaysia (Anpuanandam et al., 2021),
49 United Kingdom (Jeanes et al., 2022), United States (Stone et al., 2022), Hong Kong (Capozza et al.,
50 2023), and Japan (Takahashi et al., 2022). DCH has a partially double-stranded, circular DNA
51 genome of ~3,200 bases in length (Aghazadeh et al., 2018). As observed with other
52 *Orthohepadnavirus* species, the genome of DCH encodes polymerase, surface, core, and X proteins.
53 However, the viral replication process of DHC is largely unknown, especially the entry into target
54 cells.

55 HBV uses three envelope glycoproteins: Large (preS1 + preS2 + S), Middle (preS2 + S), and
56 Small (S only) proteins for infection. Notably, the myristoylated preS1 domain is responsible for

57 interaction with the cellular receptor (Engelke et al., 2006; Gripon et al., 2005; Le Seyec et al., 1999;
58 Schulze et al., 2010). NTCP, a sodium-dependent bile acid symporter, is the major cell receptor for
59 HBV (Yan et al., 2012). Therefore, considerable effort has been made to interrupt the interaction
60 between preS1 and NTCP to develop an entry inhibitor. Myrcludex B, a synthetic lipopeptide
61 derived from the preS1 domain of the HBV envelope protein, specifically targets hepatocytes to
62 efficiently block de novo HBV infection (Gripon et al., 2005; Schulze et al., 2010), and has
63 consequently received approval in Europe to treat patients.

64 In this study, we sought to use DCH as a model for HBV infection and investigated the entry
65 pathway of DCH using the DCH-derived preS1 peptide. We demonstrated that the DCH-derived
66 preS1 peptide efficiently binds to cat, and importantly, human NTCP. Consistent with findings with
67 HBV (Takeuchi et al., 2019), the G158 residue of NTCP determines the species specificity of DCH,
68 suggesting that the binding mode of preS1 and NTCP is conserved between HBV and DCH and that
69 there is a potential risk of inter-species transmission of DCH. Myrcludex B potently inhibited
70 binding of the DCH-derived preS1 peptide to human and cat NTCPs, suggesting that mode of
71 inhibition can be evaluated in DCH-infected cats. Overall, this study provides a promising strategy
72 for establishing a novel animal model for HBV infection, which could help develop therapeutic
73 measures in HBV-infected individuals.

74 **2. Materials and Methods**

75

76 **2.1. Plasmids**

77 NTCP cDNA sequences of 19 animal species (**Table. 1**) were synthesized (Twist Bioscience) with
78 codon optimization for expression in human cells. Synthesized DNA sequences are summarized in
79 **Supplementary Table 1**. For transient expression of NTCP, inserts encoding NTCP cDNA were
80 cloned into a pCAGGS vector (Niwa et al., 1991) predigested with EcoRI-HF (NEB, Cat# R3101M)
81 and NheI-HF (NEB, Cat# R3131M) using In-Fusion Snap Assembly Master Mix (TaKaRa, Cat#
82 Z8947N). In addition, for stable expression of NTCP, inserts encoding NTCP cDNA of human, cat,
83 and cynomolgus monkey were cloned into a pLVSIN-CMV Hyg vector (TaKaRa, Cat# 6182)
84 predigested with NotI-HF (NEB, Cat# R3189L) and BamHI-HF (NEB, Cat# R3136L) using In-
85 Fusion Snap Assembly Master Mix. Plasmids were amplified using NEB 5-alpha F′Iq Competent
86 *Escherichia coli* (High Efficiency) (NEB, Cat# C2992H), and isolated with PureYield Plasmid
87 Miniprep System (Promega, Cat# A1222). Sequences of all plasmids were verified using a SupreDye
88 v3.1 Cycle Sequencing Kit (M&S TechnoSystems, Cat# 063001) with a Spectrum Compact CE
89 System (Promega). The psPAX2-IN/HiBiT plasmid was a kind gift from Dr. Kenzo Tokunaga
90 (Ozono et al., 2020).

91

92 **2.2. Generation of plasmids encoding NTCPs mutants**

93 To generate NTCP mutants, mutagenesis was performed via overlapping PCR using
94 PrimeSTAR GXL DNA polymerase (TaKaRa, Cat# R050A) with the primers listed in
95 **Supplementary Table 2**. The PCR protocol consisted of 35 cycles at 98°C for 10 s, 60°C for 15 s,
96 and 68°C for 1 min, followed by 68°C for 7 min. Amplified PCR fragments encoding the intended
97 mutation were cloned into a pCAGGS vector as described above. Plasmids were verified by
98 sequencing.

99

100 **2.3. Cell culture**

101 Lenti-X 293T cells (TaKaRa, Cat# Z2180N) were cultured in Dulbecco's modified
102 Eagle medium (DMEM) (Nacalai Tesque, Cat# 08458-16) supplemented with 10% fetal
103 bovine serum and 1× penicillin–streptomycin (Nacalai Tesque, Cat# 09367-34).

104

105 **2.4. Generation of Lenti-X 293T cells stably expressing NTCP molecules**

106 To prepare an HIV-1-based lentiviral vector, Lenti-X 293T cells were cotransfected
107 with plasmids psPAX2-IN/HiBiT, pLVSIN-CMV Hyg-NTCP, and pMD2.G using TransIT-
108 293 Transfection Reagent (TaKaRa, Cat# V2700) in Opti-MEM I Reduced Serum Medium
109 (Thermo Fisher Scientific, Cat# 31985062). The supernatant was filtered 2 days after
110 transfection, and collected lentiviral vectors were used to infect Lenti-X 293T cells. Cells
111 were cultured with 500 μg/mL Hygromycin B (Nacalai Tesque, Cat# 09287-84) for 6 days.
112 Then, single-cell cloning was performed, and the expression level of NTCP in each clone was
113 evaluated by western blotting.

114

115 **2.5. preS1 peptide binding assay**

116 Lipopeptide myr-47WT, a N-terminally myristoylated peptide comprising residues
117 2 to 47 of the preS1 region of HBV, and myr-47N9K, where Asn at position 9 is substituted
118 with Lys, were synthesized by Scrum Co. (Tokyo, Japan). In addition, lipopeptide myr-47-
119 DCH-WT, an N-terminal myristoylated peptide comprising residues 2 to 47 of the preS1
120 region of DCH, and myr-47-DCH-N9K were synthesized.

121 Lenti-X 293T cells transiently expressing NTCP (3×10^6) were plated in a Celltight
122 C-1 Plate 96F plate (Wako, Cat# 631-26891). After overnight incubation, cells were
123 cotransfected with pCAGGS-NTCP plasmids together with pCAGGS-mCherry2 plasmid

124 using TransIT-293 Transfection Reagent in Opti-MEM I Reduced Serum Medium to normalize the
125 transfection efficiency. At 24 h after transfection, cells were inoculated with the corresponding
126 peptides and incubated at 37°C for 60 min. After two washes with Gibco William's E Medium
127 (Thermo Fisher Scientific, Cat# A1217601), cells were observed under the EVOS M7000 Imaging
128 System (Thermo Fisher Scientific). The cells were also analyzed via flow cytometry. The mCherry2-
129 positive population was gated, and the percentage of FAM-positive cells were analyzed using
130 FlowJo v10.8.1 (Becton, Dickinson and Company).
131
132 **2.6. Inhibition of preS1 peptide binding by Myrcludex B treatment**
133 Cells were prepared as described above and were then treated with 1000, 100, 10, 1, 0.1,
134 0.01, or 0.001 nM Myrcludex B (Selleck, Cat# P1105) at 37°C for 1 h. After two washes with
135 DMEM, cells were inoculated with FAM-labeled preS1 peptides and incubated at 37°C for 1 h. The
136 binding of FAM-labeled preS1 peptides was measured as described above. In addition, the
137 cytotoxicity of Myrcludex B was evaluated with the Cell Counting Kit-8 (Dojindo, Cat# CK04)
138 according to the manufacturer's instruction.
139
140 **2.7. Western blotting**
141 To check the expression level of NTCPs, pelleted cells were lysed in 2× Bolt LDS sample
142 buffer (Thermo Fisher Scientific, Cat# B0008) containing 2% β-mercaptoethanol (Bio-Rad, Cat#
143 1610710) and incubated at 70°C for 10 min. Expression of HA-tagged NTCPs in Lenti-X 293T cells
144 was evaluated using SimpleWestern Abby (ProteinSimple) with an anti-HA Tag (6E2) mouse
145 monoclonal antibody (CST, Cat# 2367S, ×250) and an Anti-Mouse Detection Module
146 (ProteinSimple, Cat# DM-002). In addition, the amount of input protein was measured using a Total
147 Protein Detection Module (ProteinSimple, Cat# DM-TP01).
148

149 **2.8. Alignment of the regions around residue 158 of NTCPs and phylogenetic analysis**

150 The regions around residue 158 of the NTCPs from 20 animal species were aligned
151 using the MUSCLE algorithm in MEGA X (MEGA Software). The parameters of alignment
152 were: gap open, −2.90; gap extend, 0.00; and hydrophobicity multiplier, 1.20.
153 A phylogenetic tree was built using alignment of NTCP amino acid sequences retrieved from public
154 databases and the evolutionary analysis were conducted in MEGA X (Kumar et al., 2018; Stecher et
155 al., 2020)**.** The evolutionary history was inferred using the Maximum Likelihood method and JTT
156 matrix-based mode (Jones et al., 1992)**.** Initial tree for the heuristic search were obtained by applying
157 Neighbor-Joining method to a matrix of pairwise distances estimated using JJT model. A discrete
158 Gamma distribution was used to model evolutionary rate differences among sites. The tree is drawn
159 to scale, with branch lengths measured in the number of substitutions per site.
160

161 **2.9. Calculation of identity of NTCP among animal species**

162 The identity of NTCPs among animal species was calculated using MEGA X (Kumar et al.,
163 2018; Stecher et al., 2020) with a pairwise distance matrix. Analyses were conducted using the
164 Poisson correction model. The rate variation among sites was modeled with a gamma distribution
165 (shape parameter = 5). All ambiguous positions were removed for each sequence pair (pairwise
166 deletion option).
167

168 **2.10. Statistical analysis**

169 Differences in binding between wild type and amino acid 158 mutants were evaluated using
170 unpaired, two-tailed Student's *t*-test. A $p \leq 0.05$ was considered statistically significant. Analysis was
171 performed using Prism 9 software v9.1.1 (GraphPad Software).

172 **3. Results**

173

174 **3.1. Genetic similarity of preS1 between DCH and HBV**

175 We aligned the preS1 sequence of 13 strains of DCH, five strains of HBV (genotype A, B,
176 C, D, and F), two strains of Arctic ground squirrel hepatitis B virus, one strain of woodchuck
177 hepatitis virus and those of other viruses belonging to *Orthohepadnavirus* (**Figure 1A**). As expected,
178 HBV has different clades based on the genotype (**Figure 1B**), and DCH was also distributed into
179 several clades. Notably, the DCH preS1 sequence is genetically closer to that of HBV rather than
180 that of woodchuck hepatitis virus or Arctic ground squirrel hepatitis B virus, suggesting that DCH
181 preS1 may exhibit a similar function to that of HBV preS1.

182

183 **3.2. Genetic similarity of NTCPs among mammals**

184 We next analyzed the NTCP genetic similarities between humans and other animals,
185 including cat (**Figure 2**). The phylogenetic tree shows that the feline NTCP is genetically close to
186 primates despite being in a different branch. The similarity rates of human and cat were 86% and
187 82% at the nucleotide and amino acid levels, respectively, based on the estimation of evolutionary
188 differences between sequences (**Supplementary Table 2**). Higher sequence distances were seen for
189 NTCPs from other mammal species, such as dolphin, woodchuck, ground squirrel, mouse, rat, and
190 platypus (sequence identities of <80% compared with human NTCP). Nonetheless, some mammals
191 with a higher NTCP distance from humans contained the same amino acid at position 158 (**Figure**
192 **2**).

193

194 **3.3. The DCH preS1 peptide binds to both cat and human NTCPs**

195 Myristoylated HBV preS1 peptide (47 amino acids in length) can be used to test the binding
196 of preS1 to its counterpart NTCP (Schulze et al., 2010). Therefore, we synthesized HBV and DCH

197 FAM-labeled, myristoylated preS1 peptides. Lenti-X 293T cells transiently expressing
198 either human NTCP (HumanNTCP) or cat NTCP (CatNTCP) were tested for binding to
199 myristoylated preS1 peptides. To distinguish between transfected and untransfected cells,
200 we cotransfected a plasmid encoding mCherry2 fluorescent protein (**Figure 3A**) and
201 measured the number of FAM-positive cells in the mCherry2-positive population, which
202 should express each NTCP molecule, via fluorescent microscopy or flow cytometry
203 (**Supplementary Figure 1**). The expression level of HA-tagged NTCP molecules was
204 confirmed with western blotting (**Figure 3B**). We observed marginal binding of preS1
205 peptides to cells transfected with empty vector (**Figure 3C**). In contrast, the HBV-derived
206 preS1 peptide efficiently bound to cells expressing HumanNTCP (**Figures 3C and 3D**);
207 binding was not observed with HBV-derived preS1 peptide harboring the N9K substitution
208 (**Figure 3D**), which is consistent with previous studies demonstrating that the N9 residue is
209 critical for interaction with HumanNTCP (Yan et al., 2012). Moreover, the HBV-derived
210 preS1 peptide showed significant binding to CatNTCP to a level similar to that of
211 HumanNTCP. As previously described (Takeuchi et al., 2019), cynomolgus monkey NTCP
212 (CmNTCP) did not support binding of the HBV-derived preS1 peptide. Furthermore, we
213 found DCH-derived preS1 peptide efficiently bound to both CatNTCP and HumanNTCP
214 but not to CmNTCP (**Figures 3C and 3D**), which was confirmed with transiently
215 transfected cells and cells that stably expressed the corresponding NTCP molecules
216 (**Supplementary Figures 2A and 2B**). Furthermore, similar to HBV preS1 peptide, the
217 DCH-derived preS1 peptide harboring the N9K substitution failed to bind any NTCPs
218 (**Figure 3D**).
219 To better understand the species tropism of the DCH preS1 peptide, we expanded
220 our analysis to NTCP molecules from other mammals, including squirrel monkey, Nancy
221 Ma's night monkey, tiger, Geoffroy's cat, dog, horseshoe bat, black fruit bat, pig, cow,

222 dolphin, woodchuck, ground squirrel, mouse, rat, and platypus (**Figures 2 and 4A**). Notably, squirrel
223 monkey, horseshoe bat, ground squirrel, and woodchuck are natural hosts for *Orthohepadnavirus*
224 species (Magnius et al., 2020). The DCH-derived preS1 peptide bound to NTCP from a wide range
225 of mammals (**Figures 4B and 4C**). Although possible transmission cases of DCH to dogs have been
226 reported (Choi et al., 2022; Diakoudi et al., 2022), the binding of the DCH-derived preS1 peptide to
227 dog NTCP was weak.
228

229 **3.4. The G158 residue of NTCP determines species specificity of the DCH preS1 peptide**
230 **binding**

231 Previous studies demonstrated that G158 of HumanNTCP is critical for interaction with the
232 HBV-derived preS1 peptide (Takeuchi et al., 2019). To evaluate whether this applies to the DCH-
233 derived preS1 peptide, we generated mutant NTCPs including HumanNTCP (G158R), CatNTCP
234 (G158R), and CmNTCP (R158G) (**Figure 5A**). The HBV-derived preS1 peptide lost binding to
235 HumanNTCP (G158R) and CatNTCP (G158R) but acquired significant binding to CmNTCP
236 (R158G) (**Figures 5B and 5C**). Similarly, the DCH-derived preS1 peptide lost binding to
237 HumanNTCP (G158R) and CatNTCP (G158R) but showed significant binding to CmNTCP
238 (R158G) (**Figures 5B and 5C**), suggesting that the binding pattern of the DCH-derived preS1
239 peptide is similar to that of the HBV-derived preS1 peptide. The amino acid at position 158 is
240 therefore critical for binding with the DCH-derived preS1 peptide.

241 In addition to cynomolgus monkey (R158), non-G residues at this position can be found in
242 animals such as Nancy Ma's night monkey (S158), Geoffroy's cat (S158), black fruit bat (E158), pig
243 (S158), and dolphin (N158) (**Figure 2**). Binding analyses demonstrated that these NTCPs do not
244 support binding to either the HBV-derived or the DCH-derived preS1 peptides (**Figures 4B and 4C**).
245 To test whether changing the residue to glycine affects the binding of the DCH-derived preS1
246 peptide, we performed a mutagenesis experiment to introduce G158 to each of these NTCPs (**Figure**

247 **5D**). Substitution of residue 158 with glycine significantly augmented binding using the
248 DCH-derived preS1 peptide to the HBV-derived and the DCH-derived preS1 peptides
249 (**Figure 5E**). Interestingly, unlike the HBV-derived preS1 peptide, the DCH-derived preS1
250 peptide did not show enhanced binding to the PigNTCP with S158G susbstituion. These
251 findings demonstrate that a single amino acid at position 158 determines the interaction with
252 preS1 peptide and that this dependency is shared by HBV and DCH.
253

254 **3.5. Myrcludex B treatment blocks binding of the DCH preS1 peptide to both human and cat**
255 **NTCPs**

256 Myrcludex B specifically inhibits the interaction between HBV-derived preS1 and
257 HumanNTCP (Gripon et al., 2005; Petersen et al., 2008). Therefore, we investigated the effect of
258 Myrcludex B on the interaction between the DCH-derived preS1 peptide and HumanNTCP or
259 CatNTCP (**Figure 6A**). As previously shown (Gripon et al., 2005; Petersen et al., 2008), Myrcludex
260 B efficiently blocked the interaction between the HBV-derived preS1 peptide and HumanNTCP
261 (IC_{50}: 57.55 nM) (**Figure 6B**) without any cytotoxicity (**Supplementary Figure 3**). A comparable
262 effect was observed with a combination of HBV-derived preS1 peptide and CatNTCP (IC_{50}: 54.3
263 nM), suggesting that HumanNTCP and CatNTCP share the same mode of action for Myrcludex B-
264 mediated inhibition. Notably, Myrcludex B efficiently blocked interaction between the DCH-derived
265 preS1 peptide and HumanNTCP or CatNTCP at a similar concentration (IC_{50}: 33.79 and 35.55 nM,
266 respectively) (**Figure 6B**).

267 Collectively, the HBV-derived preS1 peptide and the DCH-derived preS1 peptide
268 share the susceptibility to Myrcludex B, suggesting that these viruses depend on similar
269 molecular interactions for binding to NTCP on the cellular surface.

270 **4. Discussion**

271

272 Herein, we demonstrated a significant similarity in cellular entry receptors between HBV and DCH.
273 Both viruses utilize NTCP as a receptor, and more importantly, the HBV-derived preS1 peptide can
274 bind to cat NTCP while the DCH-derived preS1 peptide can bind to human NTCP. Furthermore, we
275 demonstrated that the DCH-derived preS1 peptide binds to NTCPs derived from a broad range of
276 animal species, suggesting that DCH can be transmitted to these animals. Finally, we demonstrated
277 that Myrcludex B inhibits interaction of the DCH-derived preS1 peptide with human and cat NTCPs,
278 suggesting that DCH can be used for evaluation of entry inhibitors targeting HBV.

279 The phylogenetic tree of the preS1 sequence of *Orthohepadnavirus* species suggests that
280 several strains of DCH are genetically closer to HBV than orthohepadnaviruses associated with other
281 host species. This suggests that feline DCH infection can be a promising animal model for HBV
282 infection. However, infectious DCH has yet to be isolated, and this should be a focus of continued
283 research, specifically in cats. It is critical to understand whether pathogenesis of DCH in infected
284 cats causes chronic hepatitis and hepatocellular carcinoma as HBV infection can do in humans.
285 Furthermore, although an analysis based on a naturally infected cat suggested a low possibility of
286 sexual transmission of DCH, this should be evaluated under controlled experimental conditions.

287 We identified CatNTCP as a binding molecule for the preS1 peptide of DCH (**Figures 3C**
288 **and 3D**), suggesting that CatNTCP is a cellular receptor for DCH. Furthermore, mutagenesis of
289 glycine at NTCP position 158 to arginine caused a loss in binding to the DCH-derived preS1 peptide
290 for both HumanNTCP (G158R) or CatNTCP (G158R) but produced significant binding to CmNTCP
291 (R158G) (**Figures 5B and 5C**), indicating the shared nature of the binding of DCH- and HBV-
292 derived preS1 peptide to the NTCP receptors. Furthermore, DCH may be zoonotic in some
293 circumstances as the DCH-derived preS1 peptide efficiently bound to NTCPs from a broad animal
294 species, including humans (**Figure 3D and 4D**). However, infectious DCH culture is required to

295 enable testing of DCH replication in human cells. Interestingly, DogNTCP did not support
296 binding of the HBV-derived and the DCH-derived preS1 peptides (**Figure 3D**). Although
297 DCH has been identified in dogs (Diakoudi et al., 2022), the low level of expression of
298 DogNTCP in our system might contribute to this discrepancy and should be evaluated in
299 future experiments.

300 Myrcludex B efficiently inhibited interaction of the DCH-derived preS1 peptide with
301 CatNTCP (**Figure 6B**), suggesting that Myrcludex B can be used for treating cats chronically
302 infected with DCH. Furthermore, clinical information from DCH-infected cats may provide
303 insights for control of HBV infection and eliminating DCH from persistently infected cats
304 could contribute to advances in HBV cure.

305 A previous study demonstrated that several amino acids of NTCP were under positive
306 selection (Takeuchi et al., 2019), suggesting that NTCP has been a frontline for cell invasion
307 by viruses, especially hepadnaviruses. Intriguingly, CmNTCP encodes R158 to provide
308 escape from infection with HBV. We demonstrated that non-G residue were present at amino
309 acid 158 of NTCP in several animal species (**Figure 2A**), and it would be interesting to
310 investigate whether these species are natural hosts for *Orthohepadnavirus* and, if so, whether
311 coevolution of their preS1 sequence has occurred to compensate for the decreased binding
312 caused by the non-G residue at NTCP position 158. Another possible evolutionary tactic
313 would be use of a different receptor molecule to infect the host in these species. We believe
314 testing these possibilities will provide important insights on the arms race between
315 hepadnaviruses and mammals.

316 The HBV-like virus has been identified in pigs (Vieira et al., 2014). However, the
317 genetic distance between HBV and HBV-like virus in pig is very close, and this may be a
318 possible contamination of viral DNA from HBV-infected humans. Our analysis demonstrated
319 that the HBV-derived preS1 peptide did not bind to PigNTCP, supporting this hypothesis.

320 Alternatively, the HBV-like virus in pigs may carry other mutations in the preS1 domain for efficient
321 binding with PigNTCP harboring S158. Considering a risk of food-borne transmission, whether pigs
322 are a host for *Orthohepadnavirus* species should be investigated.

323 A limitation of this study is that we used synthesized lipopeptides to test the interaction
324 between preS1 and the NTCP molecule and investigate the viral entry pathway. Therefore, the
325 interaction between the DCH-derived preS1 peptide and NTCPs require experimental verification
326 using infectious virus. Consequently, we are currently trying to isolate infectious DCH. We believe
327 future study using infectious DCH will support our present findings.

328 In conclusion, we revealed a significant similarity in the cell entry pathway between HBV
329 and DCH, suggesting a potential risk of inter-species transmission. Furthermore, our finding that
330 Myrcludex B is active against both HBV and DCH suggests that the DCH infection in cats can be a
331 promising animal model for HBV research.

332

333 **Glossary**

334 - DCH: Domestic cat hepadnavirus
335 - HBV: Hepatitis B virus
336 - MEGA: Molecular Evolutionary Genetics Analysis

337

338 **References**

339 Aghazadeh, M., Shi, M., Barrs, V.R., McLuckie, A.J., Lindsay, S.A., Jameson, B., Hampson, B.,
340 Holmes, E.C., Beatty, J.A., 2018. A Novel Hepadnavirus Identified in an
341 Immunocompromised Domestic Cat in Australia. Viruses 10, 269.
342 https://doi.org/10.3390/v10050269
343 Anpuanandam, K., Selvarajah, G.T., Choy, M.M.K., Ng, S.W., Kumar, K., Ali, R.M., Rajendran,
344 S.K., Ho, K.L., Tan, W.S., 2021. Molecular detection and characterisation of Domestic Cat
345 Hepadnavirus (DCH) from blood and liver tissues of cats in Malaysia. BMC Vet Res 17, 9.
346 https://doi.org/10.1186/s12917-020-02700-0
347 Capozza, P., Carrai, M., Choi, Y.R., Tu, T., Nekouei, O., Lanave, G., Martella, V., Beatty, J.A.,
348 Barrs, V.R., 2023. Domestic Cat Hepadnavirus: Molecular Epidemiology and Phylogeny in
349 Cats in Hong Kong. Viruses 15, 150. https://doi.org/10.3390/v15010150
350 Choi, Y.R., Chen, M.-C., Carrai, M., Rizzo, F., Chai, Y., Tse, M., Jackson, K., Martella, V., Steiner,
351 J., Pesavento, P.A., Beatty, J.A., Barrs, V.R., 2022. Hepadnavirus DNA Is Detected in
352 Canine Blood Samples in Hong Kong but Not in Liver Biopsies of Chronic Hepatitis or
353 Hepatocellular Carcinoma. Viruses 14, 1543. https://doi.org/10.3390/v14071543
354 Delmas, J., Schorr, O., Jamard, C., Gibbs, C., Trépo, C., Hantz, O., Zoulim, F., 2002. Inhibitory
355 effect of adefovir on viral DNA synthesis and covalently closed circular DNA formation in
356 duck hepatitis B virus-infected hepatocytes in vivo and in vitro. Antimicrob Agents
357 Chemother 46, 425–433. https://doi.org/10.1128/AAC.46.2.425-433.2002
358 Diakoudi, G., Capozza, P., Lanave, G., Pellegrini, F., Di Martino, B., Elia, G., Decaro, N., Camero,
359 M., Ghergo, P., Stasi, F., Cavalli, A., Tempesta, M., Barrs, V.R., Beatty, J., Bányai, K.,
360 Catella, C., Lucente, M.S., Buonavoglia, A., Fusco, G., Martella, V., 2022. A novel
361 hepadnavirus in domestic dogs. Sci Rep 12, 2864. https://doi.org/10.1038/s41598-022-06842-
362 z
363 Engelke, M., Mills, K., Seitz, S., Simon, P., Gripon, P., Schnölzer, M., Urban, S., 2006.
364 Characterization of a hepatitis B and hepatitis delta virus receptor binding site. Hepatology
365 43, 750–760. https://doi.org/10.1002/hep.21112
366 Gripon, P., Cannie, I., Urban, S., 2005. Efficient inhibition of hepatitis B virus infection by acylated
367 peptides derived from the large viral surface protein. J Virol 79, 1613–1622.
368 https://doi.org/10.1128/JVI.79.3.1613-1622.2005
369 Guo, J.T., Zhou, H., Liu, C., Aldrich, C., Saputelli, J., Whitaker, T., Barrasa, M.I., Mason, W.S.,
370 Seeger, C., 2000. Apoptosis and regeneration of hepatocytes during recovery from transient
371 hepadnavirus infections. J Virol 74, 1495–1505. https://doi.org/10.1128/jvi.74.3.1495-
372 1505.2000
373 Jeanes, E.C., Wegg, M.L., Mitchell, J.A., Priestnall, S.L., Fleming, L., Dawson, C., 2022.
374 Comparison of the prevalence of Domestic Cat Hepadnavirus in a population of cats with
375 uveitis and in a healthy blood donor cat population in the United Kingdom. Vet Ophthalmol
376 25, 165–172. https://doi.org/10.1111/vop.12956
377 Jilbert, A.R., Wu, T.T., England, J.M., Hall, P.M., Carp, N.Z., O'Connell, A.P., Mason, W.S., 1992.
378 Rapid resolution of duck hepatitis B virus infections occurs after massive hepatocellular
379 involvement. J Virol 66, 1377–1388. https://doi.org/10.1128/JVI.66.3.1377-1388.1992
380 Jones, D.T., Taylor, W.R., Thornton, J.M., 1992. The rapid generation of mutation data matrices
381 from protein sequences. Comput Appl Biosci 8, 275–282.
382 https://doi.org/10.1093/bioinformatics/8.3.275
383 Kajino, K., Jilbert, A.R., Saputelli, J., Aldrich, C.E., Cullen, J., Mason, W.S., 1994. Woodchuck
384 hepatitis virus infections: very rapid recovery after a prolonged viremia and infection of

virtually every hepatocyte. J Virol 68, 5792–5803. https://doi.org/10.1128/JVI.68.9.5792-5803.1994

Kumar, S., Stecher, G., Li, M., Knyaz, C., Tamura, K., 2018. MEGA X: Molecular Evolutionary Genetics Analysis across Computing Platforms. Mol Biol Evol 35, 1547–1549. https://doi.org/10.1093/molbev/msy096

Lanave, G., Capozza, P., Diakoudi, G., Catella, C., Catucci, L., Ghergo, P., Stasi, F., Barrs, V., Beatty, J., Decaro, N., Buonavoglia, C., Martella, V., Camero, M., 2019. Identification of hepadnavirus in the sera of cats. Sci Rep 9, 10668. https://doi.org/10.1038/s41598-019-47175-8

Le Seyec, J., Chouteau, P., Cannie, I., Guguen-Guillouzo, C., Gripon, P., 1999. Infection process of the hepatitis B virus depends on the presence of a defined sequence in the pre-S1 domain. J Virol 73, 2052–2057. https://doi.org/10.1128/JVI.73.3.2052-2057.1999

Magnius, L., Mason, W.S., Taylor, J., Kann, M., Glebe, D., Dény, P., Sureau, C., Norder, H., 2020. ICTV Virus Taxonomy Profile: Hepadnaviridae. J Gen Virol 101, 571–572. https://doi.org/10.1099/jgv.0.001415

Marion, P.L., Salazar, F.H., Winters, M.A., Colonno, R.J., 2002. Potent efficacy of entecavir (BMS-200475) in a duck model of hepatitis B virus replication. Antimicrob Agents Chemother 46, 82–88. https://doi.org/10.1128/AAC.46.1.82-88.2002

Niwa, H., Yamamura, K., Miyazaki, J., 1991. Efficient selection for high-expression transfectants with a novel eukaryotic vector. Gene 108, 193–199. https://doi.org/10.1016/0378-1119(91)90434-d

Ozono, S., Zhang, Y., Tobiume, M., Kishigami, S., Tokunaga, K., 2020. Super-rapid quantitation of the production of HIV-1 harboring a luminescent peptide tag. J Biol Chem 295, 13023–13030. https://doi.org/10.1074/jbc.RA120.013887

Petersen, J., Dandri, M., Mier, W., Lütgehetmann, M., Volz, T., von Weizsäcker, F., Haberkorn, U., Fischer, L., Pollok, J.-M., Erbes, B., Seitz, S., Urban, S., 2008. Prevention of hepatitis B virus infection in vivo by entry inhibitors derived from the large envelope protein. Nat Biotechnol 26, 335–341. https://doi.org/10.1038/nbt1389

Piewbang, C., Wardhani, S.W., Chaiyasak, S., Yostawonkul, J., Chai-In, P., Boonrungsiman, S., Kasantikul, T., Techangamsuwan, S., 2020. Insights into the genetic diversity, recombination, and systemic infections with evidence of intracellular maturation of hepadnavirus in cats. PLoS One 15, e0241212. https://doi.org/10.1371/journal.pone.0241212

Schulze, A., Schieck, A., Ni, Y., Mier, W., Urban, S., 2010. Fine mapping of pre-S sequence requirements for hepatitis B virus large envelope protein-mediated receptor interaction. J Virol 84, 1989–2000. https://doi.org/10.1128/JVI.01902-09

Stecher, G., Tamura, K., Kumar, S., 2020. Molecular Evolutionary Genetics Analysis (MEGA) for macOS. Molecular Biology and Evolution 37, 1237–1239. https://doi.org/10.1093/molbev/msz312

Stone, C., Petch, R., Gagne, R.B., Nehring, M., Tu, T., Beatty, J.A., VandeWoude, S., 2022. Prevalence and Genomic Sequence Analysis of Domestic Cat Hepadnavirus in the United States. Viruses 14, 2091. https://doi.org/10.3390/v14102091

Takahashi, K., Kaneko, Y., Shibanai, A., Yamamoto, S., Katagiri, A., Osuga, T., Inoue, Y., Kuroda, K., Tanabe, M., Okabayashi, T., Naganobu, K., Minobe, I., Saito, A., 2022. Identification of domestic cat hepadnavirus from a cat blood sample in Japan. J Vet Med Sci 84, 648–652. https://doi.org/10.1292/jvms.22-0010

Takeuchi, J.S., Fukano, K., Iwamoto, M., Tsukuda, S., Suzuki, R., Aizaki, H., Muramatsu, M., Wakita, T., Sureau, C., Watashi, K., 2019. A Single Adaptive Mutation in Sodium Taurocholate Cotransporting Polypeptide Induced by Hepadnaviruses Determines Virus Species Specificity. J Virol 93, e01432-18. https://doi.org/10.1128/JVI.01432-18

434 Vieira, Y.R., dos Santos, D.R.L., Portilho, M.M., Velloso, C.E.P., Arissawa, M., Villar, L.M., Pinto,
435 M.A., de Paula, V.S., 2014. Hepadnavirus detected in bile and liver samples from domestic
436 pigs of commercial abattoirs. BMC Microbiol 14, 315. https://doi.org/10.1186/s12866-014-
437 0315-2
438 Yan, H., Zhong, G., Xu, G., He, W., Jing, Z., Gao, Z., Huang, Y., Qi, Y., Peng, B., Wang, H., Fu, L.,
439 Song, M., Chen, P., Gao, W., Ren, B., Sun, Y., Cai, T., Feng, X., Sui, J., Li, W., 2012.
440 Sodium taurocholate cotransporting polypeptide is a functional receptor for human hepatitis
441 B and D virus. Elife 1, e00049. https://doi.org/10.7554/eLife.00049
442

443

Acknowledgements

The authors thank Dr. Toru Okamoto (Osaka University) for insightful suggestions. The following reagents were obtained through the Addgene: pMD2.G was a gift from Dr. Didier Trono. The psPAX2-IN/HiBiT plasmid was a kind gift from Dr. Kenzo Tokunaga. The authors thank Ms. Tomoko Nishiuchi and Ms. Yuki Shibatani for their assistance. Figures 2, 3A and 6A were created with BioRender (https://biorender.com/).

Author information

Contributions

M.S. and A.S. designed experiments. M.S., A.O., and A.S. performed experiments. M.S. Y.K., and A.S. analyzed results. M.S. and A.S. wrote manuscript. All authors read and approve the manuscript.

Data availability

Source data available on request.

Funding

This work was supported by grants from the Japan Agency for Medical Research and Development (AMED) Research Program on HIV/AIDS JP22fk0410033 and JP22fk0410047 (to A.S.); AMED Research Program on Emerging and Re-emerging Infectious Diseases JP21fk0108425, JP21fk0108465, and JP21fk0108481 (to A.S.); AMED Japan Program for Infectious Diseases Research and Infrastructure JP22wm0325009 (to A.S.); AMED CRDF Global Grant JP22jk0210039 (to A.S.); from JSPS KAKENHI Grant-in-Aid for Scientific Research (B) 22H02500 (to A.S.) and from the Ito Foundation Research Grant R4 (to A.S.).

Ethics declarations

Competing Interests

The authors declare no competing interests.

Corresponding author

Akatsuki Saito.

474 **Figure legends**

475

476 **Figure 1. Sequence alignment and phylogenetic analysis of the preS1 amino acids of**

477 **orthohepadnaviruses**

478 (A) Amino acid sequences of the preS1 domain of DCH aligned with the corresponding regions of

479 other *Orthohepadnavirus* species. Residue numbering was based on HBV genotype D strain.

480 (B) A phylogenetic tree built using alignment of preS1 amino acid sequences derived from

481 orthohepadnaviruses retrieved from public databases. The evolutionary history was inferred using

482 the Neighbor-Joining method. The percentage of replicate trees where the associated taxa clustered

483 together in the bootstrap test (1,000 replicates) are shown next to the branches.

484

485 **Figure 2. Sequence alignment of mammalian NTCP (residue 156–166) and phylogenetic**

486 **analysis of the entire mammalian NTCP sequence**

487 Mammalian NTCP amino acids (156–166) were aligned and the phylogenetic tree of the entire

488 mammalian NTCP sequence was constructed. The residue numbering was based on the human

489 NTCP sequence as a reference.

490

491 **Figure 3. DCH preS1 peptide binds to both CatNTCP and HumanNTCP.**

492 (A) Schematic overview of the binding assay of FAM-labeled preS1 peptides to Lenti-X 293T cells

493 cotransfected with human, cat, or cynomolgus monkey NTCPs and mCherry-expressing plasmid. For

494 analyses with a fluorescent microscopy or a flow cytometer, the presence of FAM-positive cells in

495 the mCherry2-positive population was analyzed.

496 (B) Expression levels of human, cat, or cynomolgus monkey NTCPs in transiently transfected Lenti-

497 X 293T cells was examined via western blotting

498 (C) Cells were inoculated with HBV or DCH-derived preS1 peptides harboring wild-type amino
499 acids or N9K substitution. HumanNTCP-expressing cells without the HBV-derived preS1 peptide
500 and normal cells with the HBV-derived preS1 peptide were negative controls.
501 (D) Binding of HBV or DCH-derived preS1 peptides to NTCPs was measured via flow cytometry.
502
503 **Figure 4. Binding spectrum of the DCH-derived preS1 to mammalian NTCPs.**
504 (A) Expression levels of mammalian NTCPs in transiently transfected Lenti-X 293T cells examined
505 via western blotting.
506 (B) Cells were inoculated with HBV or DCH-derived preS1 peptides harboring wild-type amino
507 acids or N9K substitution. HumanNTCP-expressing cells without the HBV-derived preS1 peptide
508 and normal cells with the HBV-derived preS1 peptide were negative controls.
509 (C) Binding of HBV or DCH-derived preS1 peptides to the NTCPs measured via flow cytometry.
510
511 **Figure 5. The G158 residue of NTCP determines species specificity of the DCH preS1 peptide**
512 **binding.**
513 (A) Expression levels of human (G158, WT; G158R), Cat (G158, WT; G158R), cynomolgus
514 monkey (R158, WT; R158G) NTCPs in transiently transfected Lenti-X 293T cells examined via
515 western blotting
516 (B) Cells were inoculated with HBV or DCH-derived preS1 peptides harboring wild-type amino
517 acids or N9K substitution. HumanNTCP-expressing cells without the HBV-derived preS1 peptide
518 and normal cells with the HBV-derived preS1 peptide were negative controls.
519 (C) Binding of HBV or DCH-derived preS1 peptides to the NTCPs measured via flow cytometry. The
520 results are presented as the mean and standard deviation of triplicate measurements from one assay,
521 and they are representative of at least three independent experiments. Differences in binding between

522 wild type and amino acid 158 mutants were evaluated using unpaired, two-tailed Student's *t*-test.
523 ****$p < 0.0001$, ***$p < 0.001$.
524 (D) Expression levels of Nancy Ma's night monkey (S158, WT; S158G), Geoffroy's cat (S158, WT;
525 S158G), pig (S158, WT; S158G), black fruit bat (E158, WT; E158G) NTCPs in transiently
526 transfected Lenti-X 293T cells examined via western blotting.
527 (E) Cells were inoculated with the HBV or DCH-derived preS1 peptides harboring wild-type amino
528 acids or N9K substitution. HumanNTCP-expressing cells without the HBV-derived preS1 peptide and
529 normal cells with the HBV-derived preS1 peptide were negative controls. The results are presented as
530 the mean and standard deviation of triplicate measurements from one assay, and they are representative
531 of at least three independent experiments. Differences in binding between wild type and amino acid
532 158 mutants were evaluated using unpaired, two-tailed Student's *t*-test. ****$p < 0.0001$, **$p < 0.01$,
533 *$p < 0.05$.
534
535 **Figure 6. Myrcludex B treatment blocks binding of the DCH preS1 peptide to both human and**
536 **cat NTCPs.**
537 (A) Schematic overview of the Myrcludex B-mediated inhibition assay using FAM-labeled PreS1
538 peptides to Lenti-X 293T cells cotransfected with human or cat NTCPs and a mCherry-expressing
539 plasmid. For analyses with a fluorescent microscopy or a flow cytometer, the presence of FAM-
540 positive cells in the mCherry2-positive population was analyzed.
541 (B) Myrcludex B inhibits the binding of HBV or DCH-derived preS1 peptides to human or cat
542 NTCPs; IC_{50} values were calculated.

543 **Table 1. NTCP amino acid sequence of 19 animal species tested in this study**

Species	**Common name**	**GenBank Acc. No**
Homo sapiens	Human	NP 003040.1
Macaca fascicularis	Cynomolgus monkey	XP 045252552.1
Saimiri sciureus	Squirrel monkey	ALX72398.1
Aotus nancymae	Nancy Ma`s night monkey	XP 012293622.1
Felis catus	Cat	XP 003987831.1
Panthera tigris	Tiger	XP 007095203.2
Leopardus geoffroyi	Geoffroyi's cat	XP 045304082.1
Canis lupus familiaris	Dog	XP 537494.2
Tupaia belangeri	Treeshrew	AFK93890.1
Rhinolopus ferrumequinum	Horseshoe bat	KAF6352409.1
Pteropus alecto	Black fruit bat	XP 006915243.1
Sus scrofa	Pig	XP 001927730.1
Bos taurus	Cattle	NP 001039804.1
Tursiops truncates	Dolphin	XP 033706895.1
Marmota monax	Woodchuck	XP 046316751.1
Incidomys tridecemlineatus	Ground squirrel	XP 005322900.1
Mus musculus	Mouse	NP 001171032.1
Rattus novegicus	Rat	NP 058743.1
Ornithorhycus anatinus	Platypus	XP 028932136.1

544

545

Figure 1

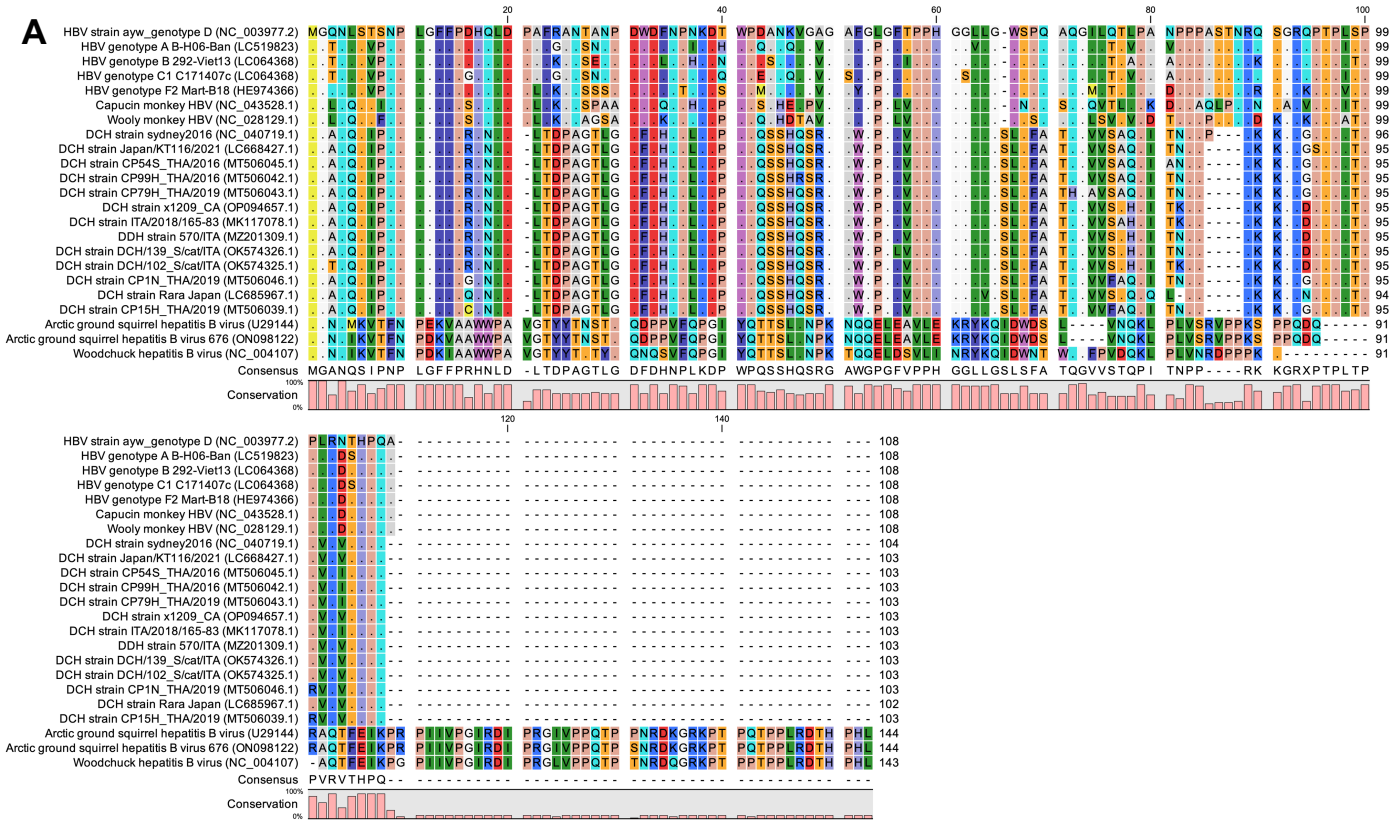
A
HBV strain ayw_genotype D (NC_003977.2)
HBV genotype A B-H06-Ban (LC519823)
HBV genotype B 292-Viet13 (LC064368)
HBV genotype C1 C171407c (LC064368)
HBV genotype F2 Mart-B18 (HE974366)
Capucin monkey HBV (NC_043528.1)
Wooly monkey HBV (NC_028129.1)
DCH strain sydney2016 (NC_040719.1)
DCH strain Japan/KT116/2021 (LC668427.1)
DCH strain CP54S_THA/2016 (MT506045.1)
DCH strain CP99H_THA/2016 (MT506042.1)
DCH strain CP79H_THA/2019 (MT506043.1)
DCH strain x1209_CA (OP094657.1)
DCH strain ITA/2018/165-83 (MK117078.1)
DDH strain 570/ITA (MZ201309.1)
DCH strain DCH/139_S/cat/ITA (OK574326.1)
DCH strain DCH/102_S/cat/ITA (OK574325.1)
DCH strain CP1N_THA/2019 (MT506046.1)
DCH strain Rara Japan (LC685967.1)
DCH strain CP15H_THA/2019 (MT506039.1)
Arctic ground squirrel hepatitis B virus (U29144)
Arctic ground squirrel hepatitis B virus 676 (ON098122)
Woodchuck hepatitis B virus (NC_004107)
Consensus
Conservation
100%
0%

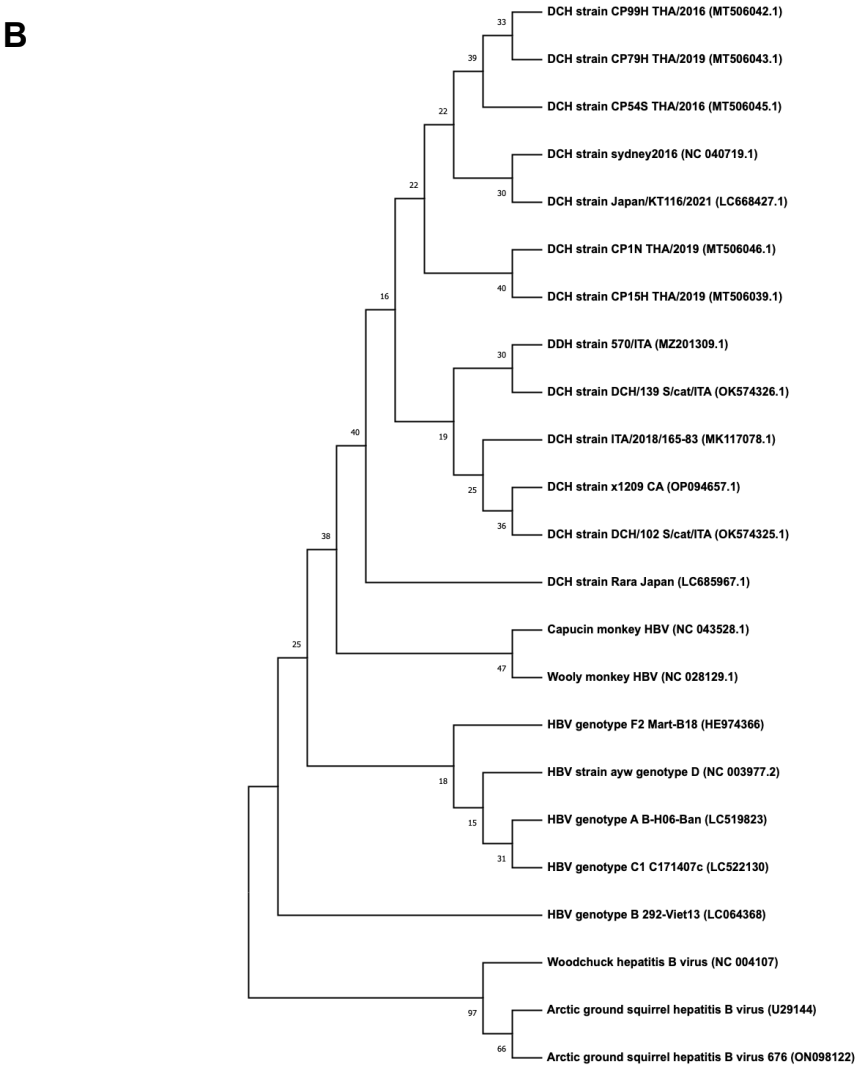
B
DCH strain CP99H THA/2016 (MT506042.1)
DCH strain CP79H THA/2019 (MT506043.1)
DCH strain CP54S THA/2016 (MT506045.1)
DCH strain sydney2016 (NC 040719.1)
DCH strain Japan/KT116/2021 (LC668427.1)
DCH strain CP1N THA/2019 (MT506046.1)
DCH strain CP15H THA/2019 (MT506039.1)
DDH strain 570/ITA (MZ201309.1)
DCH strain DCH/139 S/cat/ITA (OK574326.1)
DCH strain ITA/2018/165-83 (MK117078.1)
DCH strain x1209 CA (OP094657.1)
DCH strain DCH/102 S/cat/ITA (OK574325.1)
DCH strain Rara Japan (LC685967.1)
Capucin monkey HBV (NC 043528.1)
Wooly monkey HBV (NC 028129.1)
HBV genotype F2 Mart-B18 (HE974366)
HBV strain ayw genotype D (NC 003977.2)
HBV genotype A B-H06-Ban (LC519823)
HBV genotype C1 C171407c (LC522130)
HBV genotype B 292-Viet13 (LC064368)
Woodchuck hepatitis B virus (NC 004107)
Arctic ground squirrel hepatitis B virus (U29144)
Arctic ground squirrel hepatitis B virus 676 (ON098122)

Figure 2

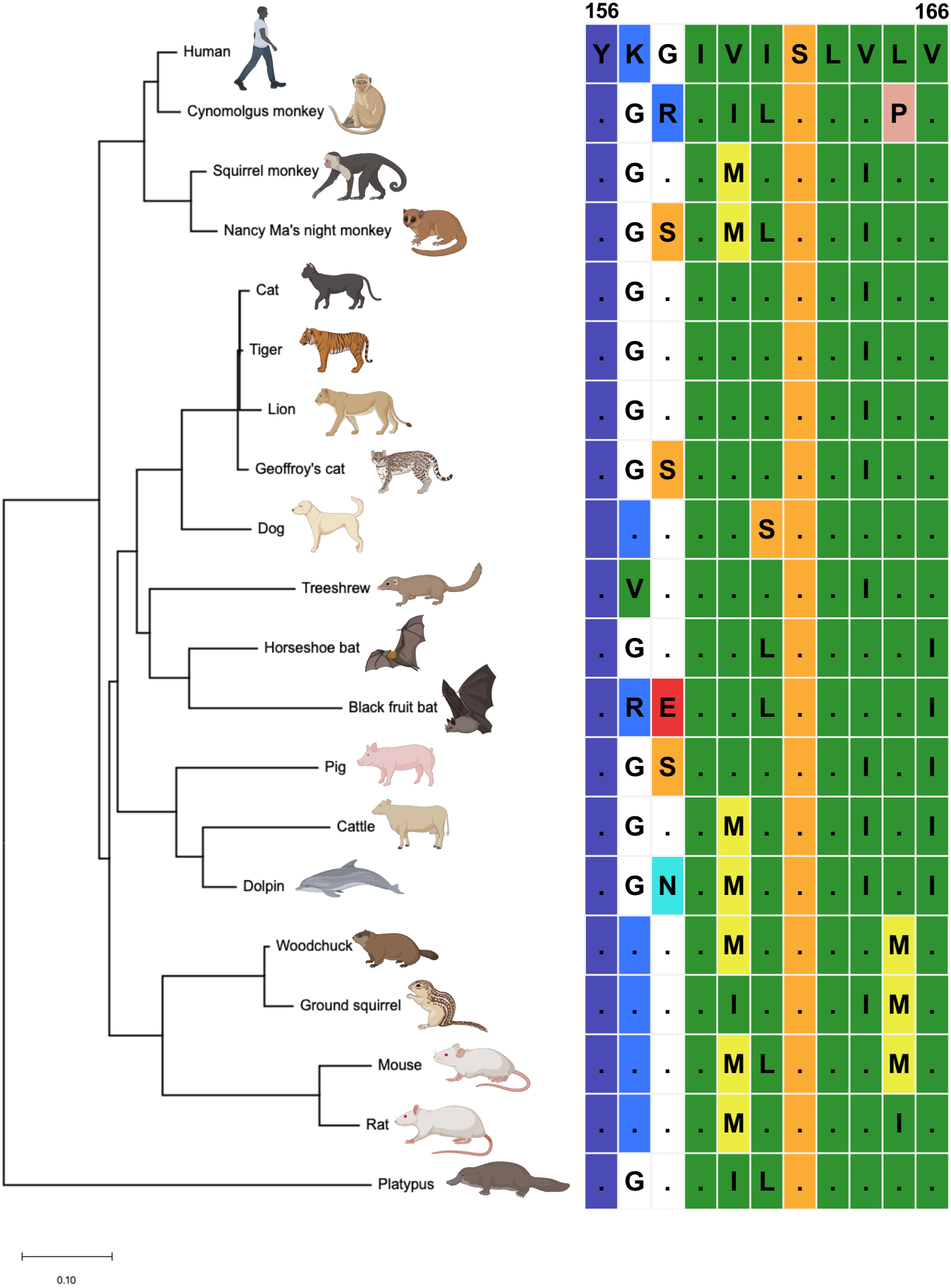
156
166
Y K G I V I S L V L V
Human
. G R . I L . . . P .
Cynomolgus monkey
. G . . M . . . I . .
Squirrel monkey
. G S . M L . . I . .
Nancy Ma's night monkey
. G . . . . . . I . .
Cat
. G . . . . . . I . .
Tiger
. G . . . . . . I . .
Lion
. G S . . . . . I . .
Geoffroy's cat
. . . . . S . . . . .
Dog
. V . . . . . . I . .
Treeshrew
. G . . . L I
Horseshoe bat
. R E . . L I
Black fruit bat
. G S . . . . . I . I
Pig
. G . . M . . . I . I
Cattle
. G N . M . . . I . I
Dolpin
. . . . M . . . . M .
Woodchuck
. . . . I . . . I M .
Ground squirrel
. . . . M L . . . M .
Mouse
. . . . M . . . . I .
Rat
. G . . I L . . . . .
Platypus
0.10

Figure 3

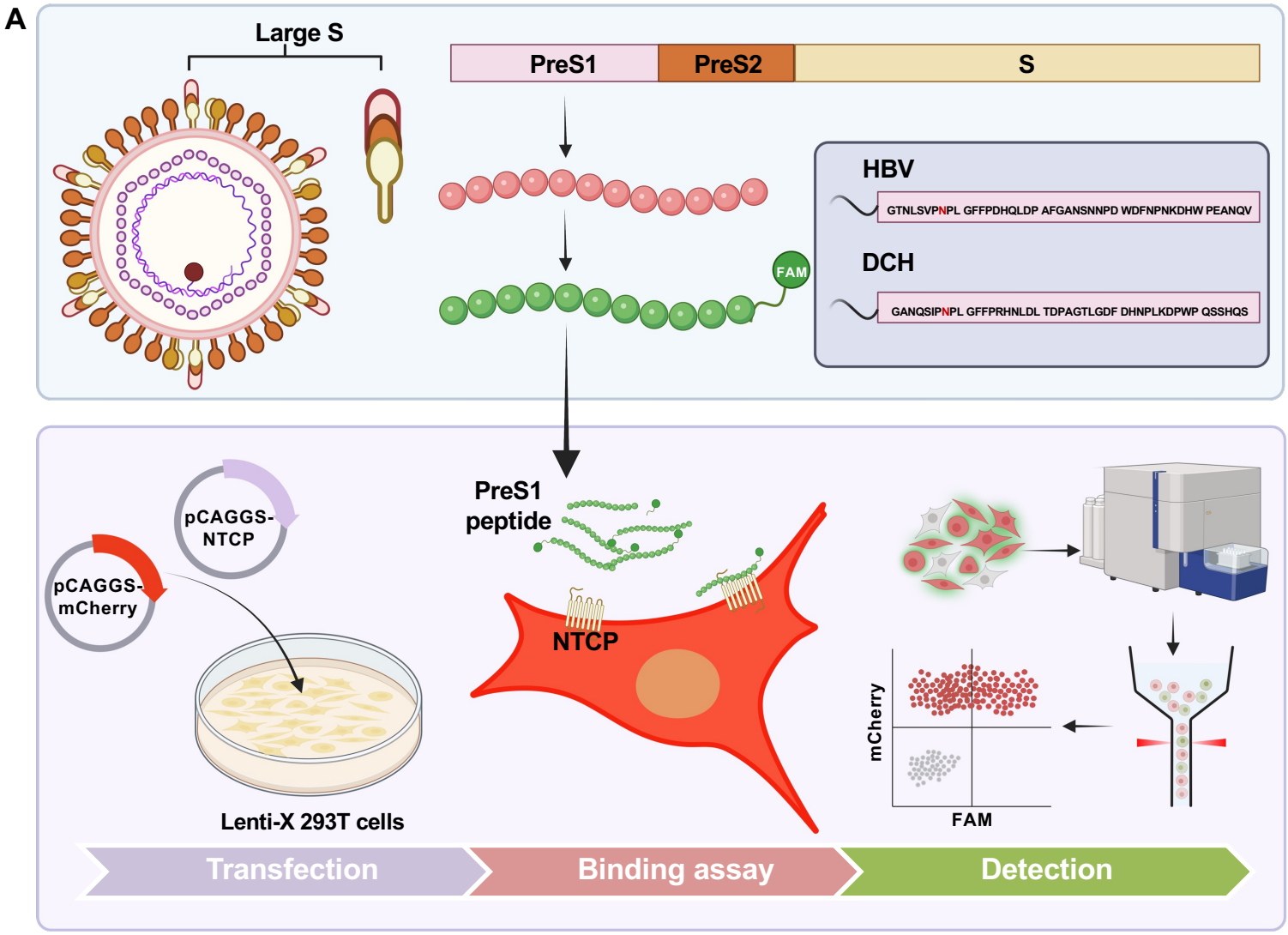
A
Large S
PreS1
PreS2
S
HBV
GTNLSVPNPL GFFPDHQLDP AFGANSNNPD WDFNPNKDHW PEANQV
DCH
GANQSIPNPL GFFPRHNLDL TDPAGTLGDF DHNPLKDPWP QSSHQS
FAM
pCAGGS-NTCP
pCAGGS-mCherry
Lenti-X 293T cells
PreS1 peptide
NTCP
mCherry
FAM
Transfection
Binding assay
Detection

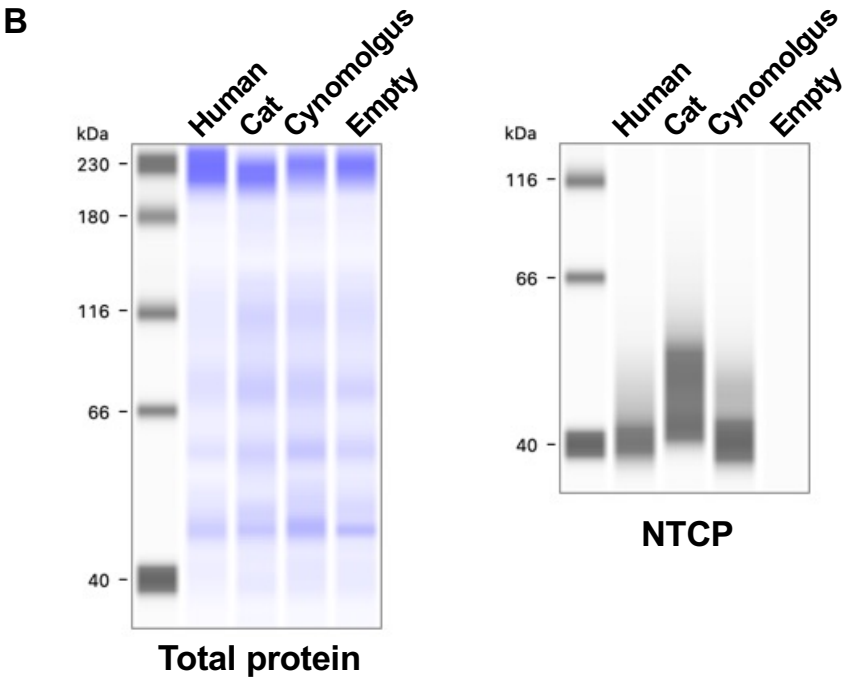
B
Human
Cat
Cynomolgus
Empty
kDa
230
180
116
66
40
Total protein
Human
Cat
Cynomolgus
Empty
kDa
116
66
40
NTCP

Figure 3 (continued)

C

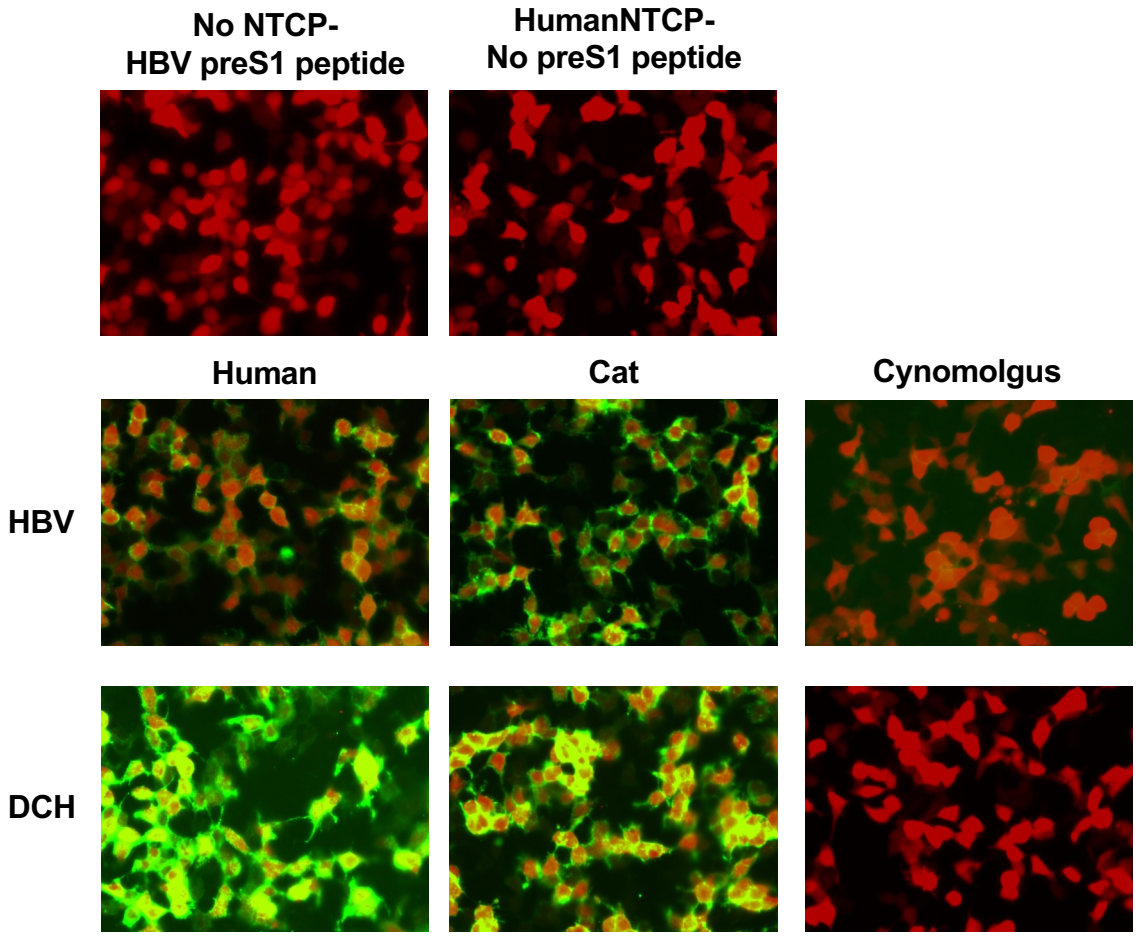

D

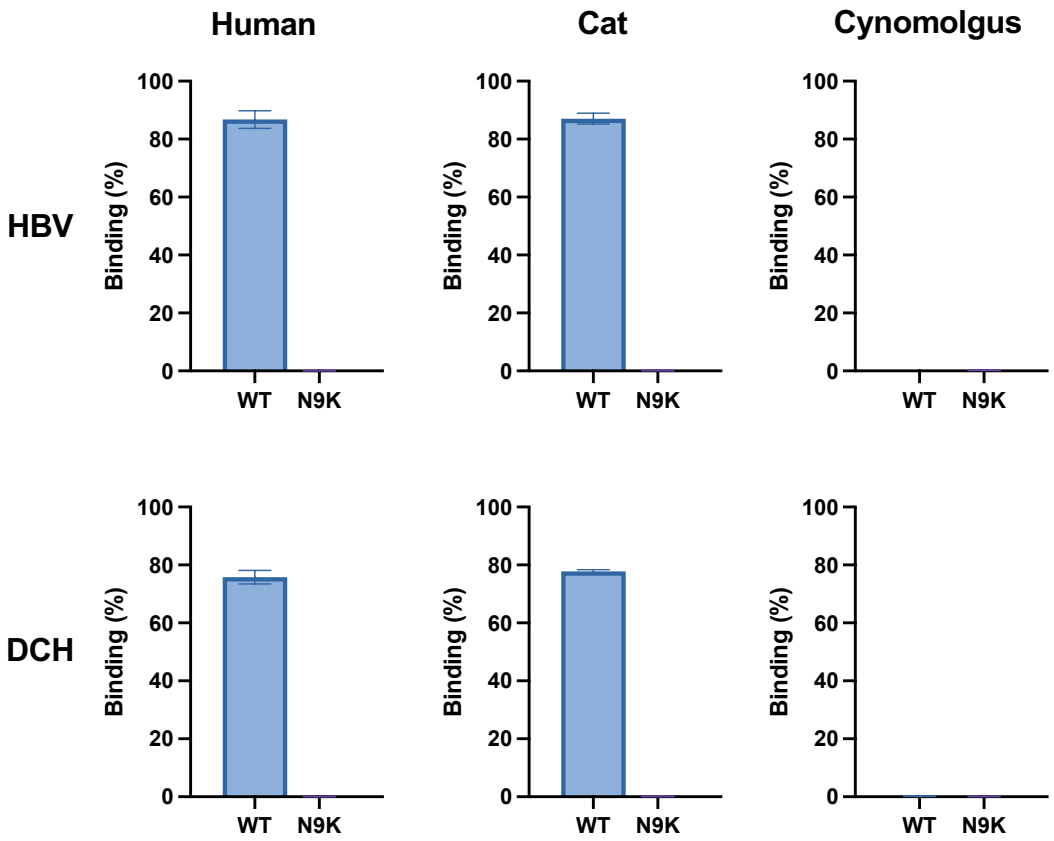

Figure 4

A

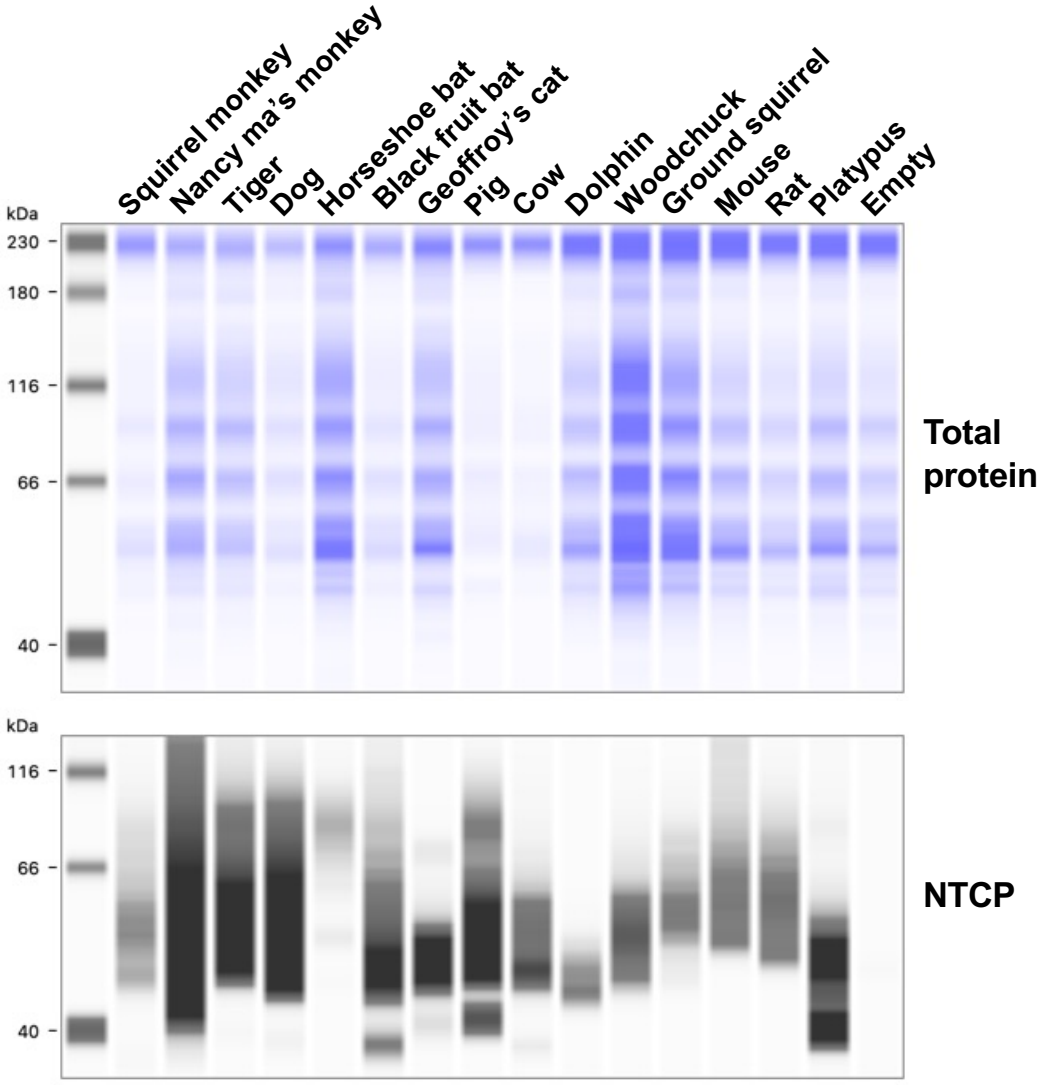
Squirrel monkey
Nancy ma's monkey
Tiger
Dog
Horseshoe bat
Black fruit bat
Geoffroy's cat
Pig
Cow
Dolphin
Woodchuck
Ground squirrel
Mouse
Rat
Platypus
Empty
kDa
230
180
116
66
40
Total protein
kDa
116
66
40
NTCP

Figure 4 (continued)

B

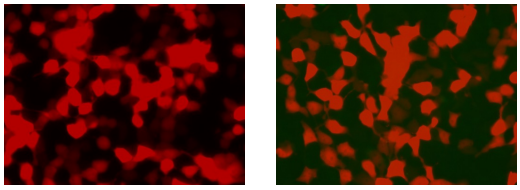

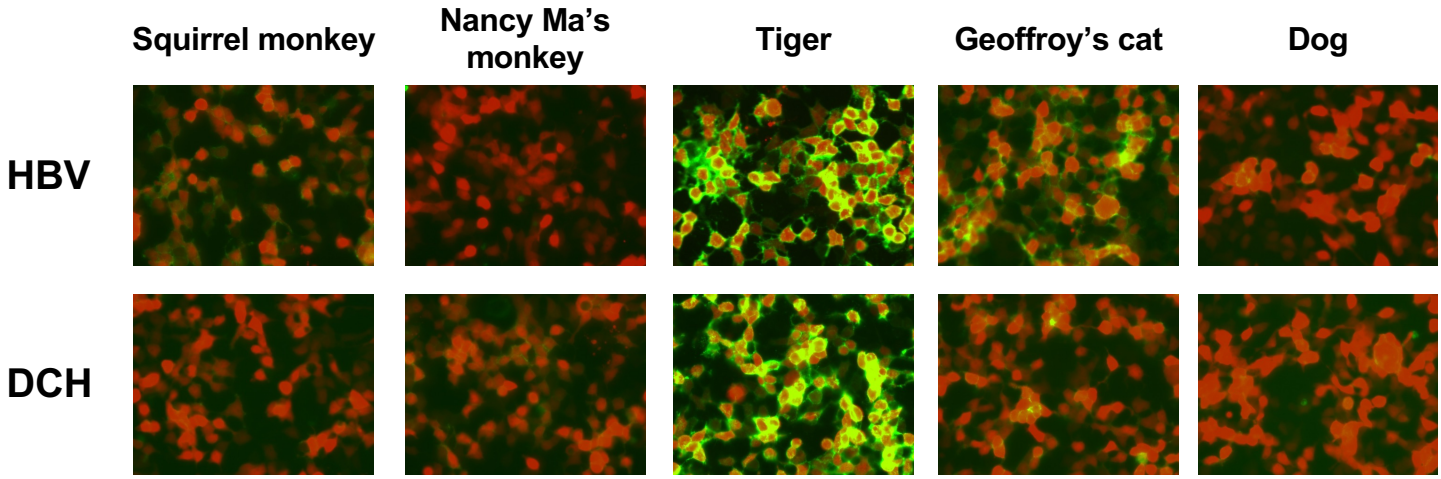

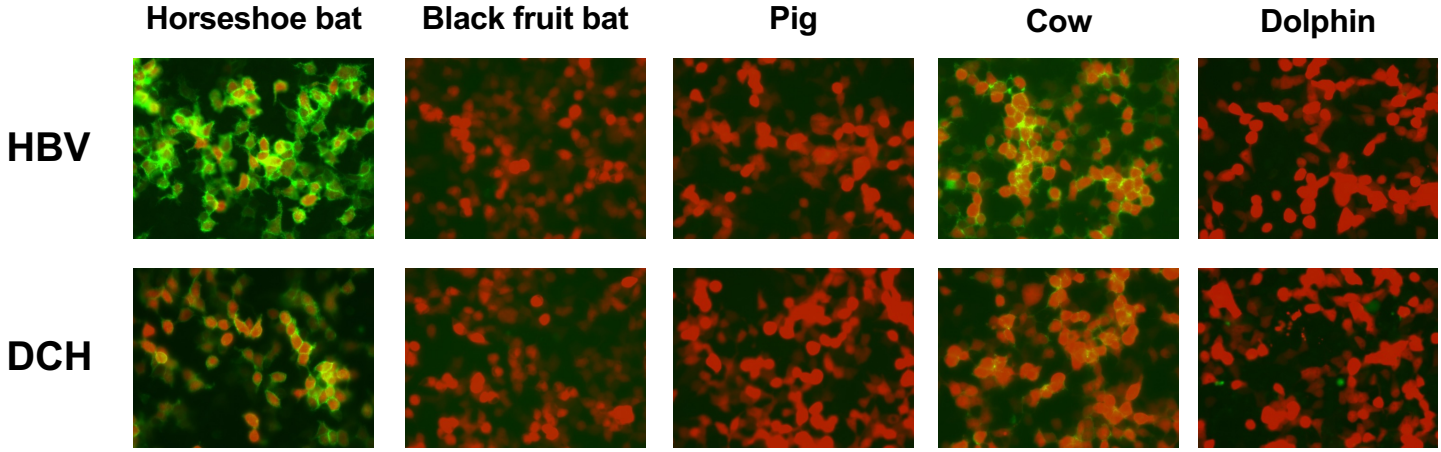

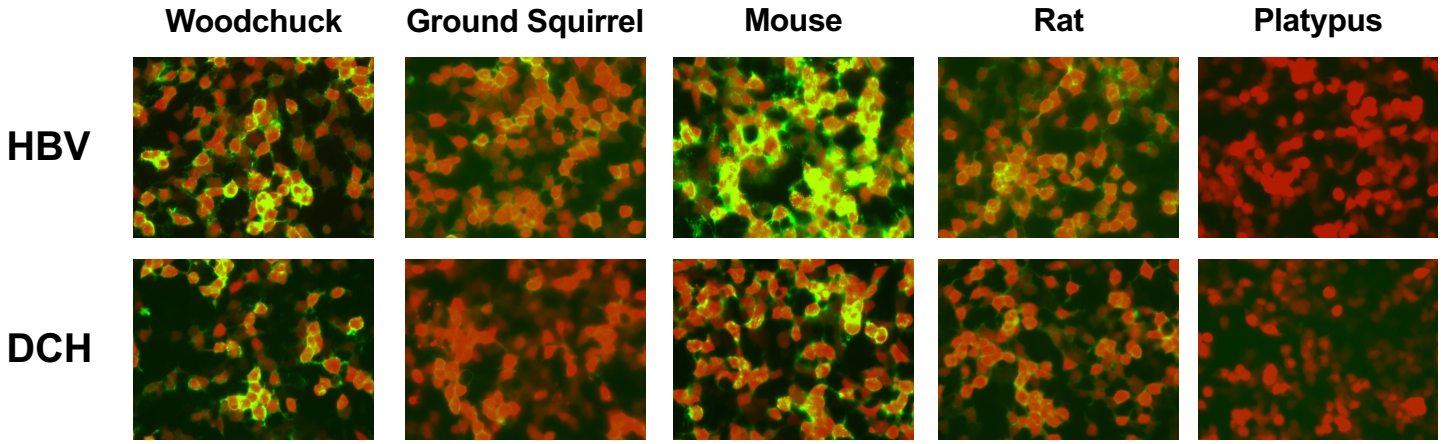

Figure 4 (continued)

C

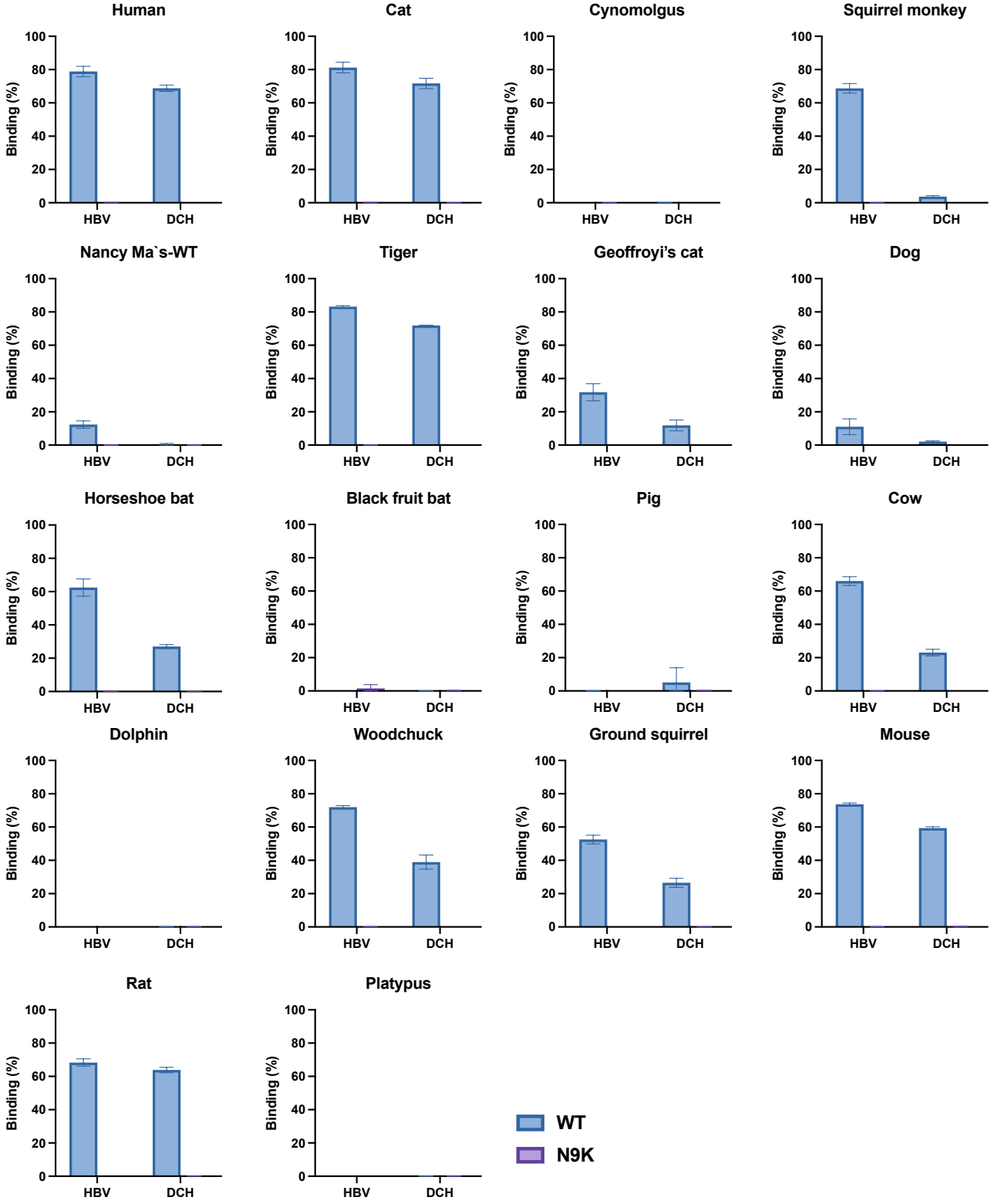

Figure 5

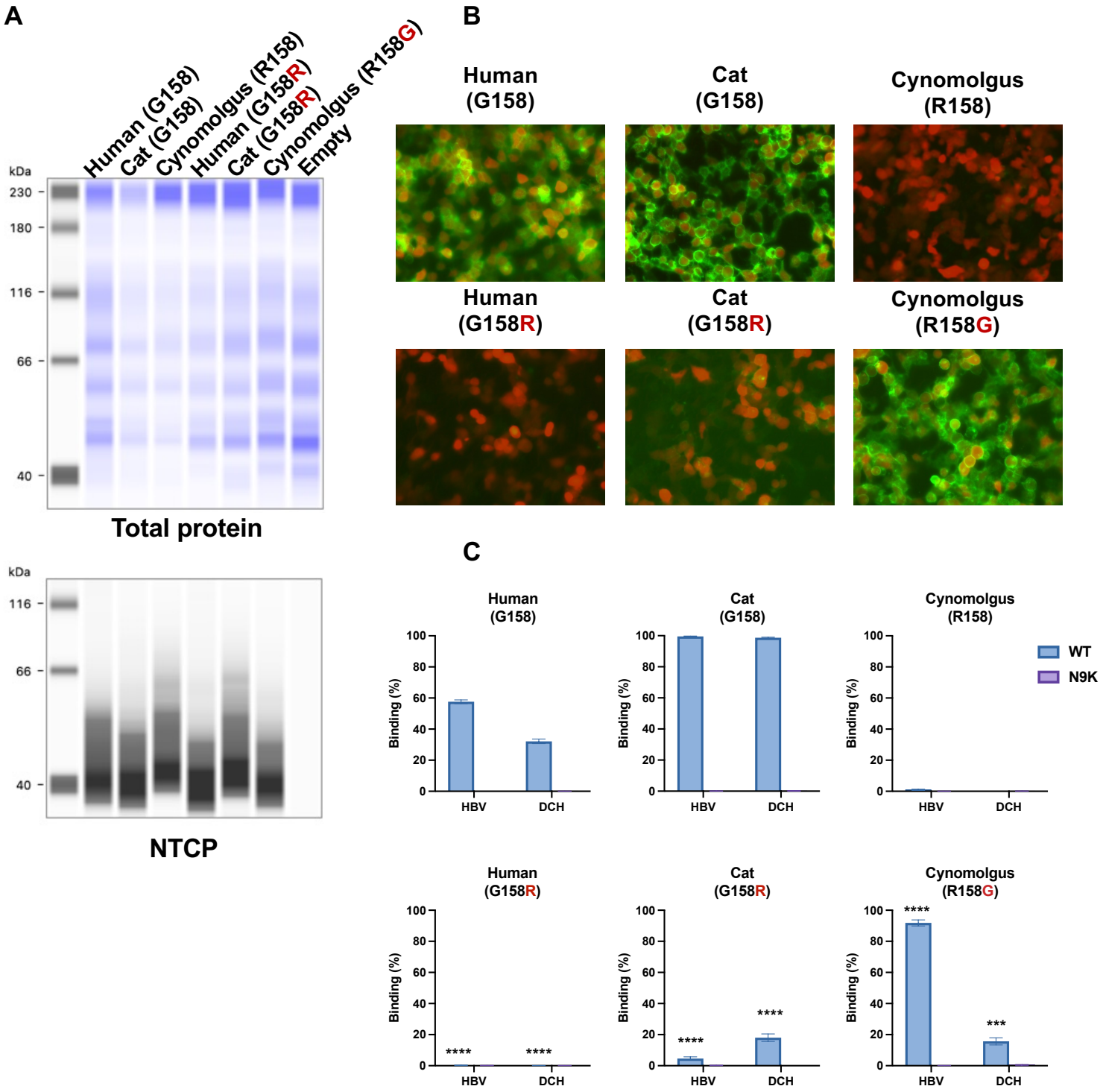
A
Human (G158)
Cat (G158)
Cynomolgus (R158)
Human (G158R)
Cat (G158R)
Cynomolgus (R158G)
Empty
kDa
230
180
116
66
40
Total protein
kDa
116
66
40
NTCP
B
Human (G158)
Cat (G158)
Cynomolgus (R158)
Human (G158R)
Cat (G158R)
Cynomolgus (R158G)
C
Human (G158)
Cat (G158)
Cynomolgus (R158)
Human (G158R)
Cat (G158R)
Cynomolgus (R158G)
Binding (%)
HBV
DCH
WT
N9K
****
***

Figure 5 (continued)

D

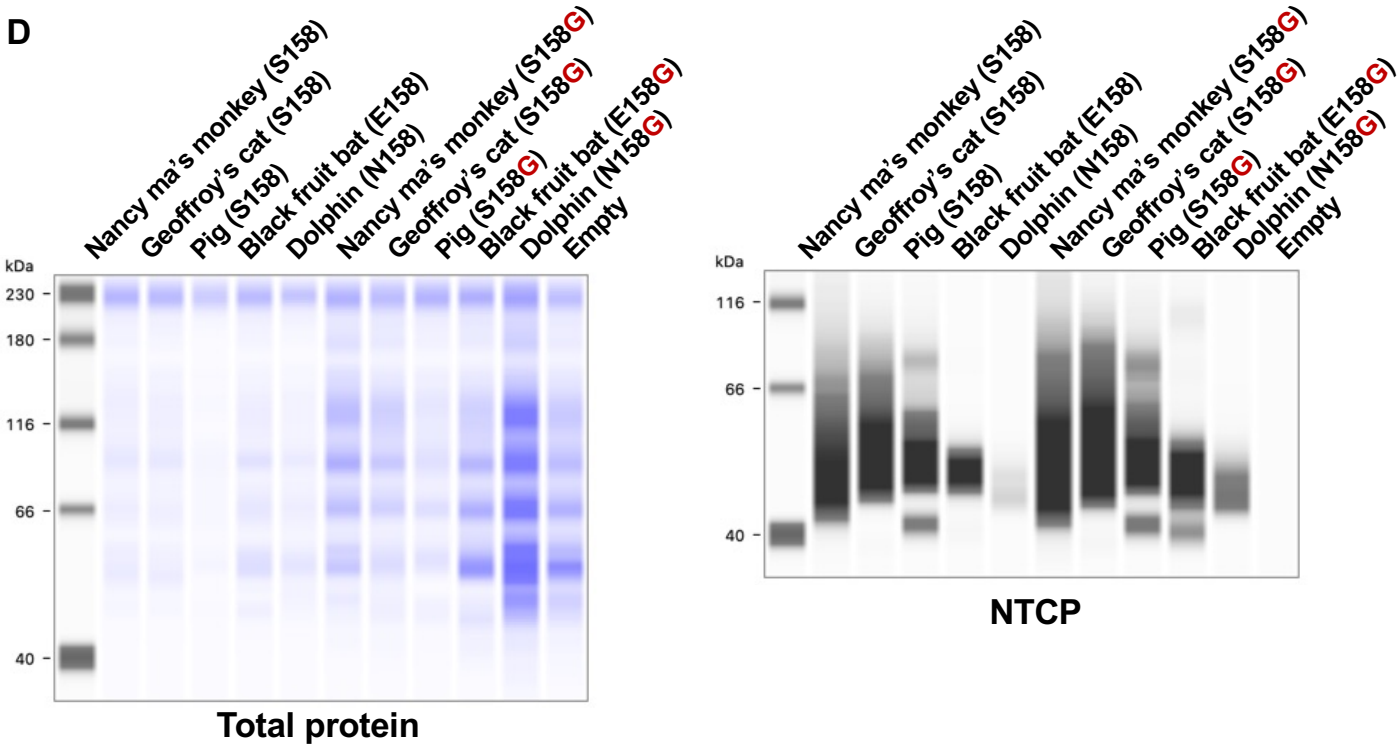

E

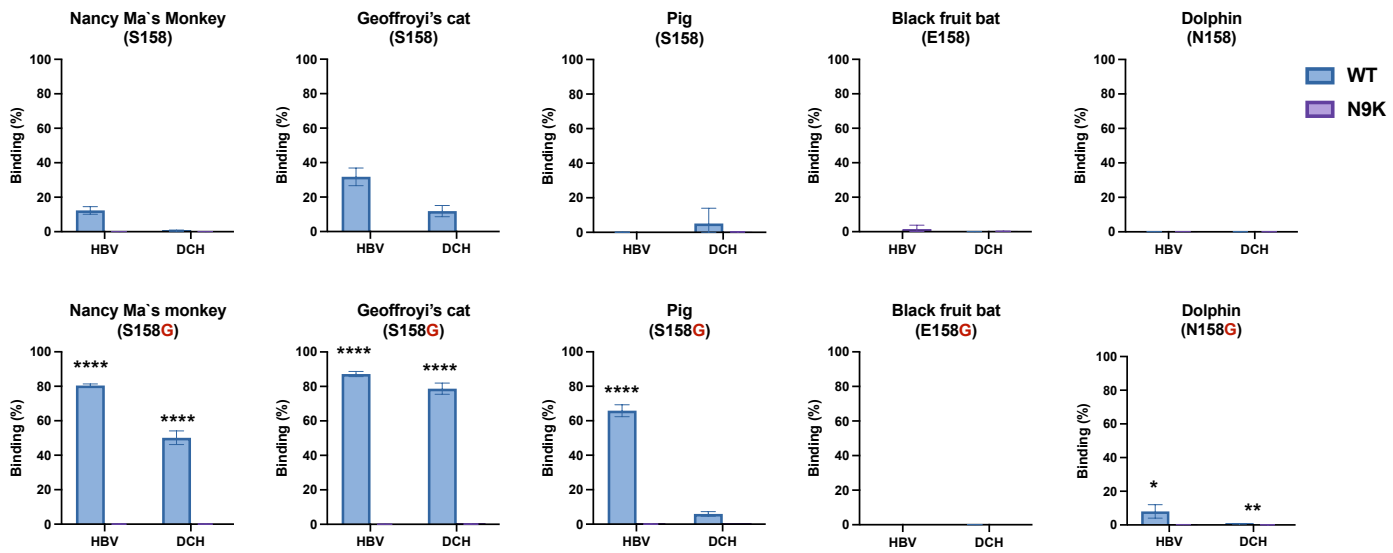

Figure 6

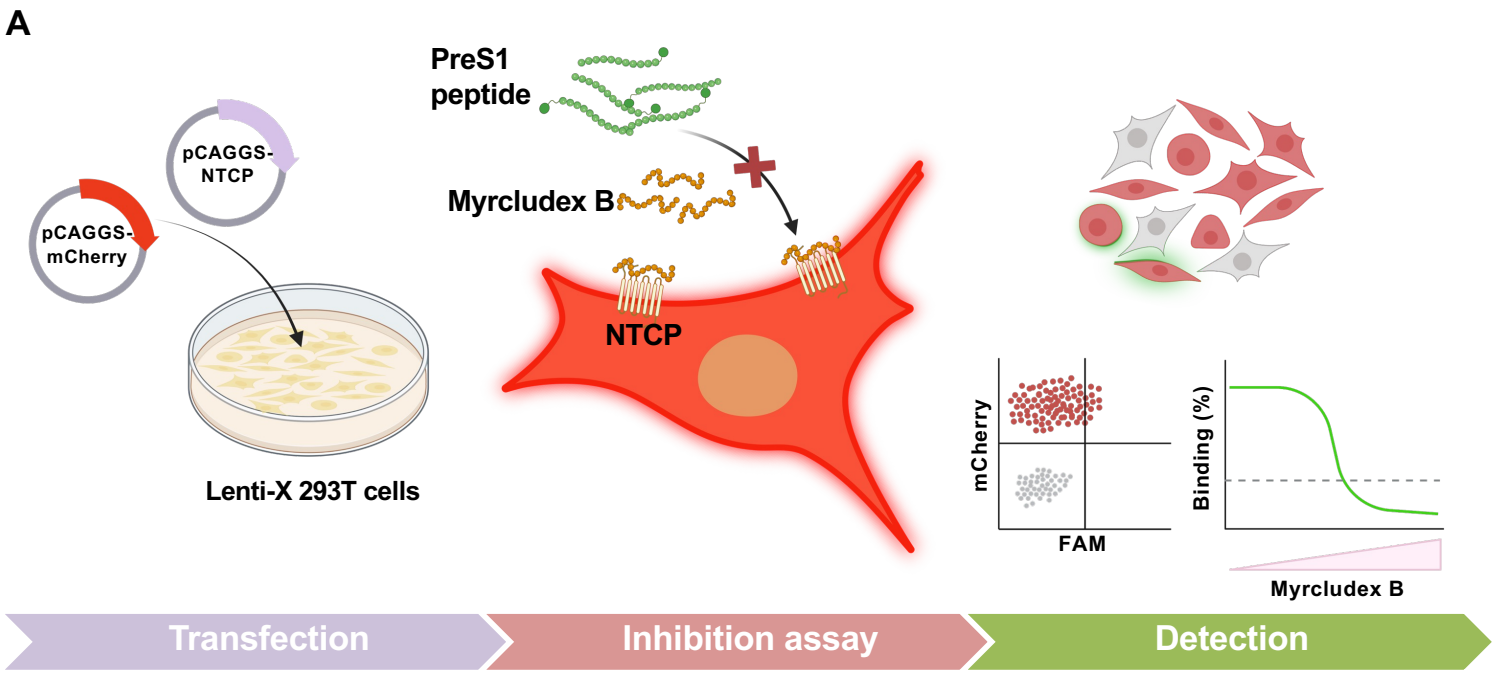
A
PreS1
peptide
pCAGGS-
NTCP
pCAGGS-
mCherry
Myrcludex B
NTCP
Lenti-X 293T cells
mCherry
FAM
Binding (%)
Myrcludex B
Transfection
Inhibition assay
Detection

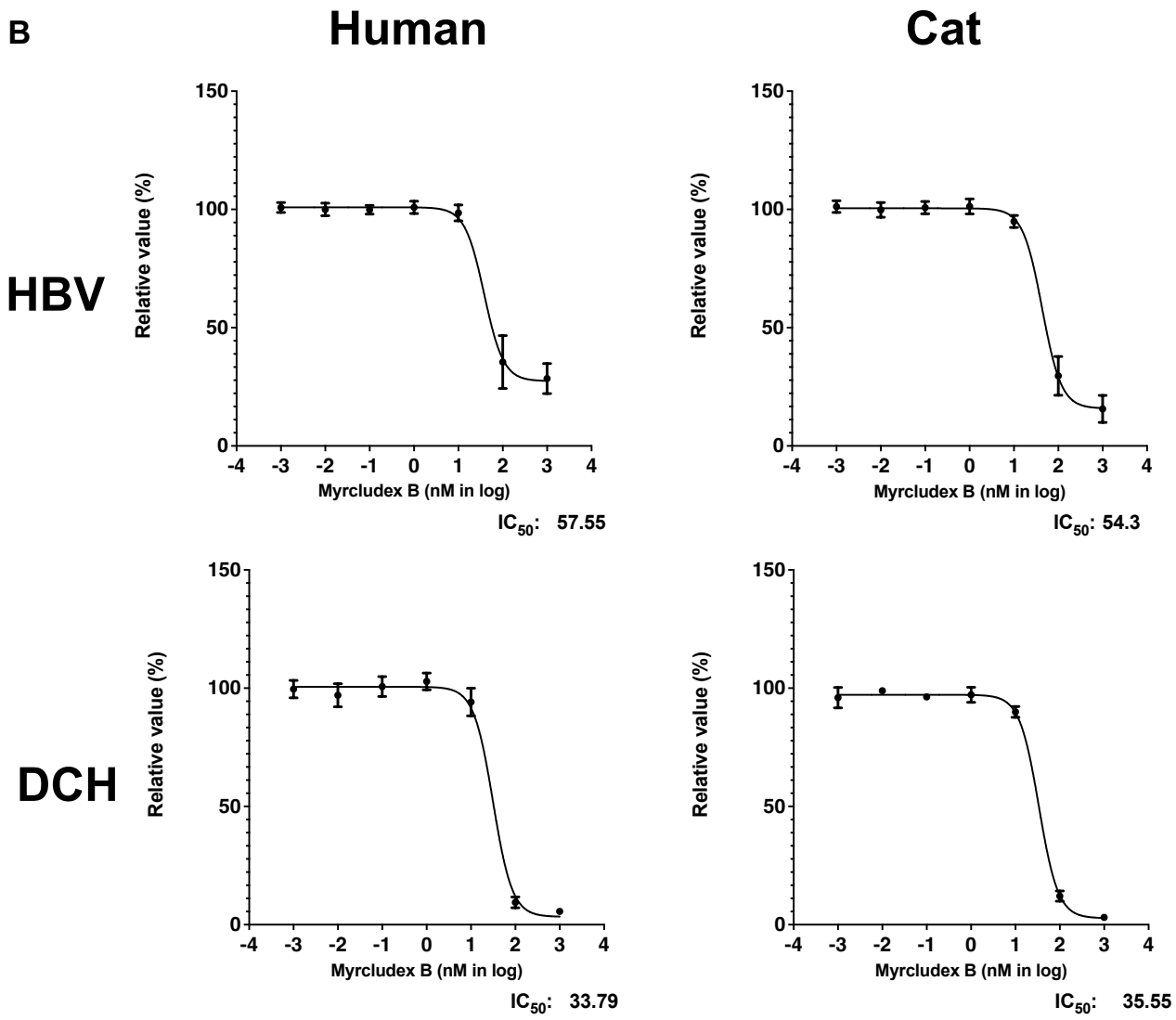
B
Human
Cat
HBV
DCH
Relative value (%)
Myrcludex B (nM in log)
IC50: 57.55
IC50: 54.3
IC50: 33.79
IC50: 35.55